CSIRO PUBLISHING

RESEARCH FRONT

Aust. J. Chem.
http://dx.doi.org/10.1071/CH16206

Full Paper

Mechanistic Insights into Water-Catalyzed Formation of Levoglucosenone from Anhydrosugar Intermediates by Means of High-Level Theoretical Procedures

Wenchao Wan,[A] *Li-Juan Yu,*[A] *and Amir Karton*[A,B]

[A]School of Chemistry and Biochemistry, The University of Western Australia, Perth, WA 6009, Australia.
[B]Corresponding author. Email: amir.karton@uwa.edu.au

Levoglucosenone (LGO) is an important anhydrosugar product of fast pyrolysis of cellulose and biomass. We use the high-level G4(MP2) thermochemical protocol to study the reaction mechanism for the formation of LGO from the 1,4:3,6-dianhydro-α-D-glucopyranose (DGP) pyrolysis intermediate. We find that the DGP-to-LGO conversion proceeds via a multistep reaction mechanism, which involves ring-opening, ring-closing, enol-to-keto tautomerization, hydration, and dehydration reactions. The rate-determining step for the uncatalyzed process is the enol-to-keto tautomerization ($\Delta G^{\ddagger}_{298} = 68.6$ kcal mol^{-1}). We find that a water molecule can catalyze five of the seven steps in the reaction pathway. In the water-catalyzed process, the barrier for the enol-to-keto tautomerization is reduced by as much as 15.1 kcal mol^{-1}, and the hydration step becomes the rate-determining step with an activation energy of $\Delta G^{\ddagger}_{298} = 58.1$ kcal mol^{-1}.

Manuscript received: 30 March 2016.
Manuscript accepted: 21 April 2016.
Published online: 24 May 2016.

Introduction

Lignocellulosic biomass – with an annual global production of 220 billion tons per year[1] – is a renewable source for fuels and chemicals and is mainly composed of cellulose, hemicellulose, and lignin.[2] Pyrolysis is a promising technology to convert biomass into char, and liquid and gaseous products that could be further upgraded to biofuels and fine chemicals.[3] Pyrolysis liquid products are a mixture of water and hundreds of low-concentration organic compounds including acids, aldehydes, anhydrosugars, and furans.[4–6] In order to produce targeted valuable industrial chemicals, it is important to understand the chemical mechanisms underlying the formation of specific chemicals during pyrolysis.

Levoglucosenone (LGO) is one of the most valuable pyrolysis products due to its unique structure and functional groups (e.g. keto, olefinic, and ether groups).[7,8] Accordingly, LGO is the starting material for a wide range of synthetic products including biologically active natural products, sugar mimetics, and agrochemicals.[9,10] It was found that 5.5 wt-% of LGO is produced via fast pyrolysis of cellulose[11] and that the yield of LGO can be increased by using a variety of catalysts including H_3PO_4,[12–14] H_2SO_4,[15] ionic liquids,[16] SO_4^{2-}/ZrO_2, and SO_4^{2-}/TiO_2.[17]

The formation of LGO during pyrolysis has been studied both theoretically and experimentally.[7,18–24] However, the molecular mechanisms underlying the formation of LGO during pyrolysis of cellulose and biomass are still largely unknown. Several precursors for the formation of LGO were proposed and investigated.[7,19,20,25] In an early experimental study, it was suggested that levoglucosan (LG) is a precursor of LGO.[7] More recently, Assary and Curtiss[19] proposed a detailed scheme of the reaction pathways for the conversion of LG into LGO using density functional theory and high-level *ab initio* procedures. The authors found that a water molecule could catalyze this transformation with an activation barrier of $\Delta H^{\ddagger}_{298} = 56.6$ kcal mol^{-1} at the G4 level. Lu et al. studied the reaction pathways for the formation of LGO from β-D-glucopyranose and cellobiose at the B3LYP/6–31+G(d,p) level of theory.[20] They found that the enol-to-keto tautomerization is the rate-determining step (RDS) for both LGO formation reactions from β-D-glucopyranose and cellobiose, with barriers of $\Delta H^{\ddagger}_{298} = 69.5$ kcal mol^{-1} and $\Delta H^{\ddagger}_{298} = 62.7$ kcal mol^{-1}, respectively.

In a recent computational investigation, Satorri[25] investigated the reaction mechanism for the conversion of LG into LGO and suggested that 1,4:3,6-dianhydro-α-D-glucopyranose (DGP) – an important anhydrosugar product (3.3 wt-%[11]) obtained from cellulose pyrolysis – might be a possible precursor for the formation of LGO. However, the reaction mechanism for the DGP-to-LGO conversion was not investigated. Fig. 1 summarizes the two pathways for the conversion of cellulose into LGO.

Nearly four decades ago, Shafizadeh et al.[26] showed that the pyrolysis of DGP under acidic conditions generated significant amounts of LGO. The authors proposed a general reaction scheme for the formation of LGO from DGP. This scheme is illustrated in Fig. 2. This scheme involves diol, triol, and tetraol intermediates; however, the reaction mechanisms leading to their formation were not discussed. In the present work, we investigate the reaction mechanism for the uncatalyzed formation of LGO from DGP in more detail using the high-level *ab-initio* G4(MP2) theory.[27] We also consider the water-catalyzed reaction and show that a water catalyst can reduce

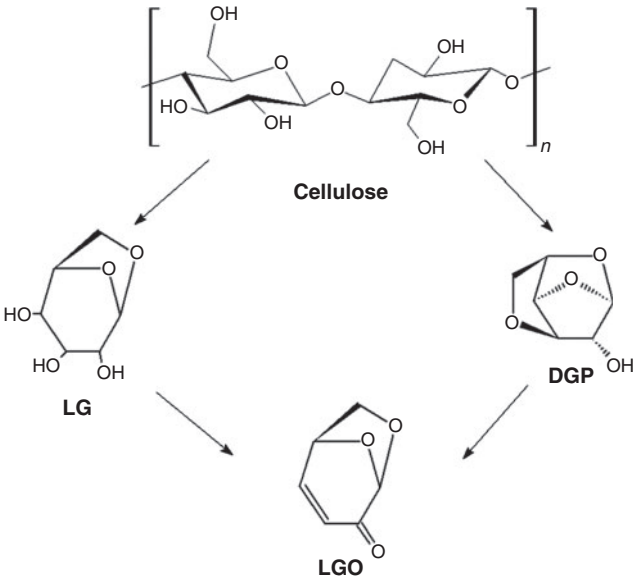

Fig. 1. Schematic of the two possible pathways for the conversion of cellulose into LGO.

the Gibbs free activation energy at 298 K ($\Delta G^{\ddagger}_{298}$) for the entire process by as much as 10.5 kcal mol^{-1}. In addition, we show that the water catalyst leads to a change in the RDS for the overall process.

Computational Methods

High-level *ab initio*[28] and density functional theory[29] calculations were carried out using the *Gaussian 09* program suite.[30] All geometry optimizations were performed at the B3LYP/6–31G(2df,p) level of theory as prescribed in the G4(MP2) protocol.[27] Zero-point vibrational energies, enthalpic, and entropic corrections have been obtained from such calculations. The equilibrium structures were verified to have all real harmonic frequencies and the transition structures to have only one imaginary frequency. The connectivities of the transition structures were confirmed by performing intrinsic reaction coordinate calculations.[31,32]

Gas-phase Gibbs free energies at 298 K (ΔG_{298}) were obtained using the G4(MP2) variant of the Gaussian-4 (G4) composite thermochemical protocol.[27,33] The G4(MP2) protocol is an efficient composite procedure for approximating the CCSD(T) (coupled cluster energy with singles, doubles, and quasiperturbative triple excitations) energy in conjunction with a large triple-ζ-quality basis set.[34,35] This protocol is widely used for the calculation of thermochemical and kinetic properties (for a recent review see Curtiss et al.[34]). The G4(MP2) procedure has been found to produce gas-phase thermochemical properties (such as reaction energies, bond dissociation energies, and enthalpies of formation) with a mean absolute deviation of 1.04 kcal mol^{-1} from the 454 experimental energies of G3/05 test set.[36] It has been recently found that G4(MP2) shows a similarly good performance for barrier heights.[37–40]

Results and Discussion

Uncatalyzed Mechanism for the Formation of LGO from DGP

Shafizadeh et al. proposed a general reaction mechanism for the conversion of DGP into LGO (Fig. 2).[26] This scheme involves

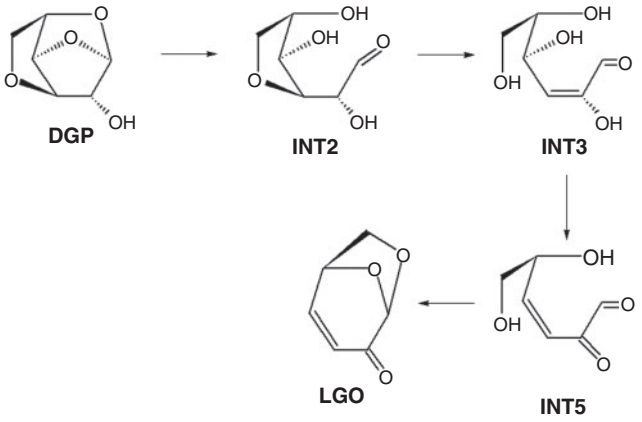

Fig. 2. Reaction scheme for the conversion of LGO into DGP proposed by Shafizadeh et al.[26] For consistency, the intermediates were labelled in the same way as in Fig. 3.

three polyol intermediates, however, the steps leading to the formation of these intermediates were not specified or discussed in detail. We begin by proposing a more detailed seven-step reaction pathway for the formation of LGO from DGP. Our proposed reaction mechanism is illustrated schematically in Fig. 3.

The seven steps in our proposed reaction mechanism are described as follows. (i) In the first step, a water molecule is added to the pyranose ring. Specifically, the hydrogen atom is added to the pyranose oxygen and a hydroxyl group is added to the C_1 carbon atom. This ring-opening reaction leads to the formation of the first intermediate (**INT1**, Fig. 3). (ii) A hydrogen-transfer reaction, in which the hydrogen from the hydroxyl group at the C_1 position is transferred to the cyclic furanose oxygen. In this step, the C_1–O bond of the furanose ring breaks, resulting in the formation of **INT2** (Fig. 3). (iii) A hydrogen-transfer from C_2 to the pyranose oxygen, leading to the breaking of the pyranose ring and the formation of an acyclic structure (**INT3**). (iv) An enol-to-keto tautomerization, leading to the formation of **INT4** (Fig. 3). (v) A dehydration reaction, in which the hydrogen attached to C_3 is eliminated with the hydroxyl group attached to C_4, leading to the formation of the C_3=C_4 bond in **INT5**. (vi) A hydrogen-transfer cyclization reaction, in which the hydrogen of the hydroxyl group at C_5 shifts to the carbonyl oxygen in the C_1 position, forming a pyranose ring. (vii) A dehydration–cyclization reaction, leading to the formation of the final LGO product (Fig. 3).

We note that Shafizadeh et al. also proposed an additional reaction mechanism (scheme 1 in Shafizadeh et al.[26]). We considered this reaction mechanism and found that the first hydrogen-transfer step has a higher Gibbs free activation energy than the RDS for the mechanism illustrated in Fig. 3. For the uncatalyzed reaction, the barrier for the first step of this alternative mechanism is $\Delta G^{\ddagger}_{298} = 73.6$ kcal mol^{-1}, whereas the barrier for the RDS for the mechanism in Fig. 3 is 68.6 kcal mol^{-1} (see below). Similarly, for the water-catalyzed reaction, the barrier for the first step of the alternative mechanism is $\Delta G^{\ddagger}_{298} = 71.1$ kcal mol^{-1}, whereas the barrier for the RDS for the mechanism in Fig. 3 is 58.1 kcal mol^{-1} (see *Water Catalyzed Mechanism for the Formation of LGO from DGP*). Therefore, we will not consider this alternative mechanism here (see Supplementary Material for further details).

The G4(MP2) Gibbs free energy profile (ΔG_{298}) for the uncatalyzed reaction pathway is depicted in Fig. 4 (black line), whereas Fig. 5 shows the optimized transition structures (TSs) located along the uncatalyzed reaction profile. The lowest

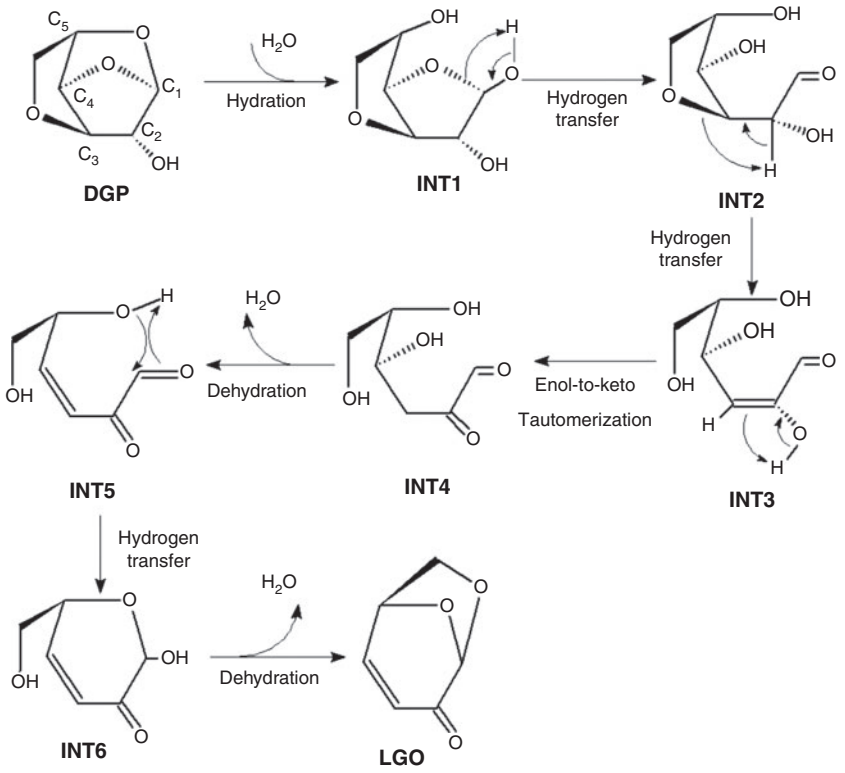

Fig. 3. Detailed reaction mechanism for the conversion of DGP into LGO proposed in the present work.

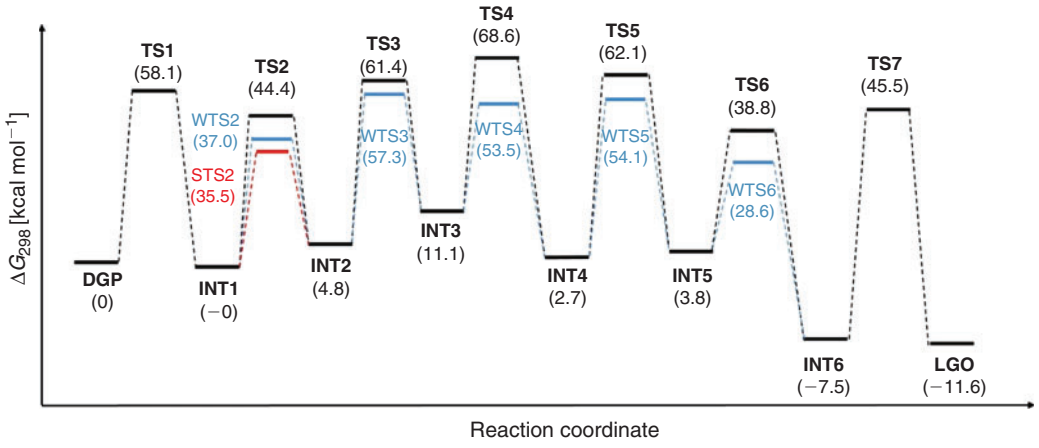

Fig. 4. Reaction profile (G4(MP2), ΔG_{298}, kcal mol^{-1}) for the uncatalyzed (black line), water-catalyzed (blue line), and self-catalyzed (red line) conversion of DGP into LGO.

energy conformation of DGP is chosen as the zero-energy reference point of the reaction profile. The first hydration step has an activation energy of $\Delta G^{\ddagger}_{298}$(**TS1**) = 58.1 kcal mol^{-1}. The relatively high activation energy for this step may be attributed to the fact that the bonds that are being broken and formed in **TS1** are far from their equilibrium distances. In particular, the bond length of the C_1–O of the pyranose ring to be broken is 2.603 Å, whereas the bond lengths of O–H and C_1–OH to be formed are 1.472 and 2.288 Å, respectively. Interestingly, the product of this hydration reaction (**INT1**) is essentially isoenergetic with the DGP reactant.

The transition structures for the succeeding five steps (**TS2**–**TS6**) share similar structural features – they all involve a strained four-membered ring formed between a migrating hydrogen atom and three heavy C and O atoms (Fig. 5). The Gibbs free activation energies for these steps spread over a wide range from 38.8 (**TS6**) to 68.6 (**TS4**) kcal mol^{-1}. The last dehydration step of the reaction mechanism is associated with a relatively low activation Gibbs free energy of $\Delta G^{\ddagger}_{298}$(**TS7**) = 45.5 kcal mol^{-1} (or $\Delta G^{\ddagger}_{298}$(**TS7**) = 53.0 kcal mol^{-1} relative to the stable **INT6** intermediate). The TSs with the highest Gibbs free activation energies are **TS3**–**TS5**. Therefore, we will now concentrate on these steps.

The TS for the ring-opening, hydrogen-transfer step (**TS3**, Fig. 5) involves a hydrogen transfer from C_2 to the furanose oxygen, breaking of the C_3–O bond, and formation of the C_2=C_3 bond. This TS has an activation energy of $\Delta G^{\ddagger}_{298}$(**TS3**) = 61.4 kcal mol^{-1}. The lengths of the C_3–O and C_2–H bonds to be

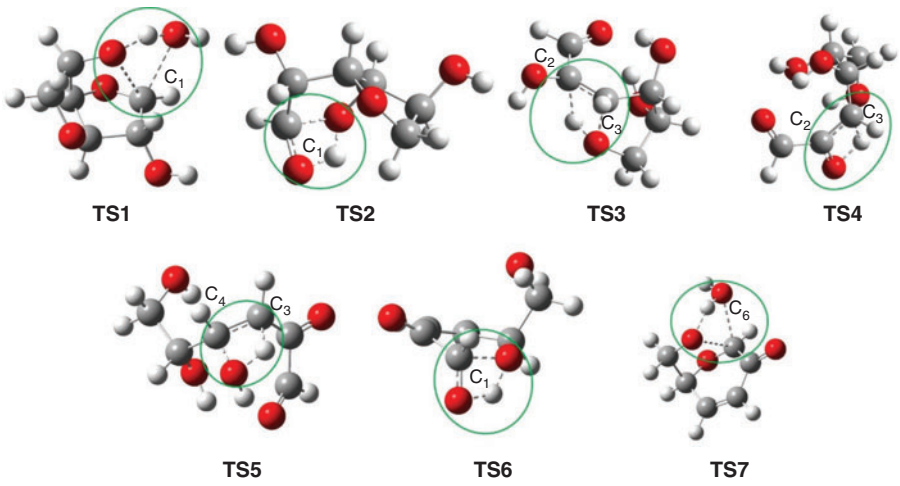

Fig. 5. B3LYP/6–31G(2df,p) optimized transition structures **TS1**–**TS7** in the reaction profile for the uncatalyzed conversion of DGP into LGO (Fig. 4). The bonds being broken and formed in the TSs are represented by dashed lines. Atomic colour scheme: H, white; C, grey; O, red. The carbon atoms involved in the TSs are labelled in the same way as in Fig. 3.

broken are 1.576 and 1.554 Å, respectively, whereas the lengths of the C_2=C_3 and O–H bonds to be formed are 1.500 and 1.175 Å, respectively.

The enol-to-keto tautomerization (**TS4**, Fig. 5) is the RDS for the entire process, with an activation Gibbs free energy of 68.1 kcal mol^{-1} relative to the DGP reactant. We note that the reaction barrier relative to the enol tautomer (**INT3**) is 57.5 kcal mol^{-1}. This reaction barrier is almost identical to the G4(MP2) reaction barrier for the enol-to-keto tautomerization in vinyl alcohol (56.9 kcal mol^{-1}).[38] It has been previously shown that this reaction can be catalyzed by a range of catalysts, including water, organic acids, and inorganic acids,[41,42] which alleviate the high strain energy involved in the TS. We also note that the G4(MP2) reaction barrier for the enol-to-keto tautomerization in vinyl alcohol is in very good agreement with the barrier height calculated at the higher W1-F12 level (56.7 kcal mol^{-1}).[41,43] This close agreement increases our confidence in the G4(MP2) reaction barrier heights.

The transition structure for the first dehydration step (**TS5**, Fig. 5) involves the elimination of the hydroxyl group at the C_3 position with the hydrogen at the C_4 position (Fig. 3). Similarly to the TSs for the 1,3-hydrogen transfer steps (**TS2**, **TS3**, **TS4**, and **TS6**), **TS5** involves a strained four-membered ring as shown in Fig. 5. In **TS5**, the hydroxyl group at the C_4 position has a strong hydrogen bond with the carbonyl oxygen at the C_1 position. This is evident from the relatively short length of the OH•••OC_1 hydrogen bond (namely 1.686 Å). The Gibbs free activation energy for this step is 62.1 kcal mol^{-1}. For comparison, this barrier is significantly lower than the uncatalyzed barrier reported by Assary et al.[19] for the initial dehydration step in the conversion of LG into LGO ($\Delta G^{\ddagger}_{298} = 68.7$ kcal mol^{-1}, MP2/6–311++G(3df,3pd)). Another point of reference is the dehydration reaction in ethanol; the G4(MP2) barrier for this reaction is $\Delta G^{\ddagger}_{298} = 66.7$ kcal mol^{-1}. The lower Gibbs free activation energy for **TS5** may be partially attributed to the above-mentioned hydrogen-bonding interaction.

The last two steps of the reaction are highly exergonic. Namely, **INT6** lies 7.5 kcal mol^{-1} below the reactant, and the final LGO product lies 11.6 kcal mol^{-1} below the reactant. Both steps are associated with relatively low reaction barrier heights of 38.8 (**TS6**) and 45.5 (**TS7**) kcal mol^{-1} (or 53.0 kcal mol^{-1} relative to the stable intermediate **INT6**).

Two important features of the overall reaction profile for the uncatalyzed conversion of DGP into LGO are as follows:

1. The enol-to-keto tautomerization step is clearly the RDS. In particular, **TS4** is higher by amounts ranging from 6.5 (**TS5**) to 29.8 (**TS6**) kcal mol^{-1} than the other TSs involved in the process.
2. The overall process is highly exergonic; the final product lies lower in energy than the reactant by 11.6 kcal mol^{-1}. This provides a thermodynamic driving force for the entire process.[44]

It is well known that the presence of water molecules can significantly enhance the reaction rates of hydrogen-transfer reactions in the gas phase relative to the rates of the uncatalyzed reactions.[38,41,42,44–47] Thus, **TS2**–**TS6**, which involve a strained four-membered ring formed between a migrating hydrogen and three heavy C and O atoms (Fig. 5), could potentially be catalyzed by a water catalyst. In the next section, we explore the water-catalyzed conversion of DGP into LGO.

Water Catalyzed Mechanism for the Formation of LGO from DGP

Water is not only a major constituent of raw biomass material,[48,49] but also a significant pyrolytic product of pyrolysis processes such as the hydroperoxide decomposition step.[50] It has been found that water could catalyze certain important reactions in the pyrolysis of glucose such as ring-opening,[51] tautomerization,[52] and dehydration reactions.[52] In this section, we investigate the reaction profile for the conversion of DGP into LGO catalyzed by a water molecule.

We find that an explicit water molecule can act as a hydrogen bridge in the transition structures **TS2**–**TS6**, thereby lowering the activation energies for these steps by amounts ranging from 4.1 (**TS3**) to 15.1 (**TS4**) kcal mol^{-1}. As a consequence of this catalytic activity, the enol-to-keto tautomerization (**TS4**) is no longer the RDS. The RDS for the catalyzed process becomes the first dehydration step (**TS1**), which cannot be catalyzed by a water molecule.

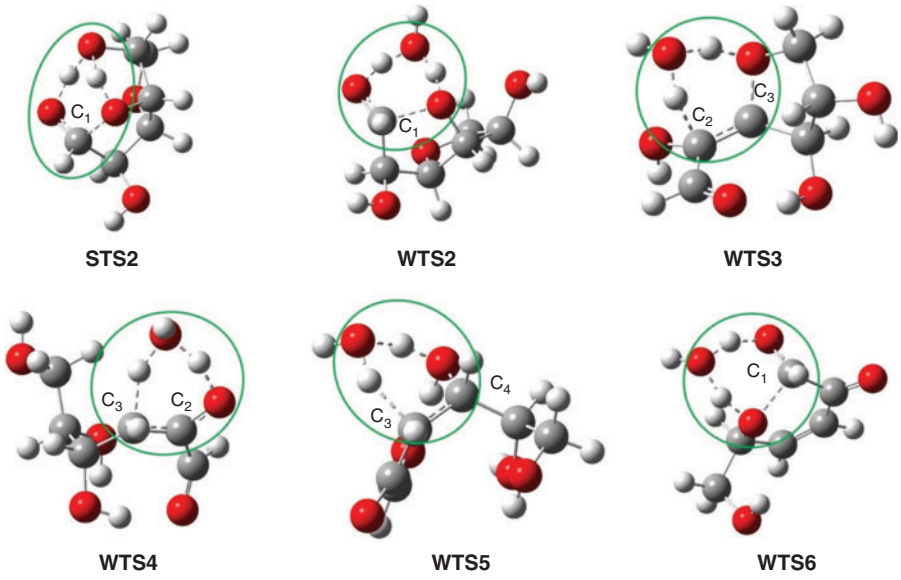

Fig. 6. B3LYP/6–31G(2df,p) optimized transition structures **TS2**–**TS6** in the reaction profile for the (self- and water-) catalyzed conversion of DGP to LGO. The catalyzed reaction profile is shown in Fig. 4. The bonds being broken and formed in the TSs are represented by dashed lines. Atomic colour scheme: H, white; C, grey; O, red. The carbon atoms involved in the TSs are labelled in the same way as in Fig. 3.

The water-catalyzed reaction profile is shown in Fig. 4 (blue line) and the optimized water-catalyzed TSs (i.e. WTSs) are depicted in Fig. 6. In all of these TSs, the water molecule assists the hydrogen-transfer reaction by converting the four-membered ring TS into a less strained six-membered ring TS (Figs. 5 and 6).

In the second step, a water molecule acts as a hydrogen shuttle that transports a hydrogen from the hydroxyl group to the furanose oxygen (**WTS2**, Fig. 6). The activation energy for the catalyzed step is reduced by 7.4 kcal mol^{-1} relative to the uncatalyzed reaction. We also located a self-catalyzed TS (STS) for this step (**STS2**, Fig. 6), which is associated with a lower activation energy of $\Delta G^{\ddagger}_{298}$(**STS2**) = 35.5 kcal mol^{-1} (red line, Fig. 4). In the self-catalyzed TS, the hydroxyl group attached to C_5 acts as the hydrogen shuttle.

The activation energy for the enol-to-keto tautomerization (**WTS4**, Fig. 6) is reduced by as much as 15.1 kcal mol^{-1} upon inclusion of the water catalyst. This step, which is the RDS of the uncatalyzed process, is now associated with an activation energy of $\Delta G^{\ddagger}_{298}$(**WTS4**) = 53.5 kcal mol^{-1}. Thus, in the catalyzed mechanism, the reaction barrier for this step is lower by 4.6 kcal mol^{-1} than the reaction barrier for the hydration step ($\Delta G^{\ddagger}_{298}$(**TS1**) = 58.1 kcal mol^{-1}). Upon inclusion of the water catalyst, the activation energy for **TS5** is reduced by 8.0 kcal mol^{-1}, whereas the reaction barrier for **TS6** is reduced by 10.2 kcal mol^{-1}.

The results above indicate that the involvement of an explicit water molecule in the hydrogen shifts significantly affects the dynamics of the overall reaction. In the uncatalyzed mechanism, the RDS is the enol-to-keto tautomerization ($\Delta G^{\ddagger}_{298}$(**TS4**) = 68.6 kcal mol^{-1}). In the catalyzed mechanism, the ring-opening hydration step becomes the RDS ($\Delta G^{\ddagger}_{298}$(**TS1**) = 58.1 kcal mol^{-1}), and the ring-opening hydrogen-transfer step is associated with a slightly lower activation energy of $\Delta G^{\ddagger}_{298}$(**WTS3**) = 57.3 kcal mol^{-1}. Overall, the involvement of the water catalyst reduces the Gibbs free activation energy for the DGP-to-LGO transformation by 10.5 kcal mol^{-1}.

Conclusions

We use the high-level *ab initio* G4(MP2) thermochemical procedures to investigate the uncatalyzed and water-catalyzed reaction mechanisms for the transformation of DGP to LGO. We draw the following conclusions:

1. The reaction mechanism has seven elementary steps including ring-opening, ring-closing, enol-to-keto tautomerization, dehydration, and hydration reactions.
2. In the uncatalyzed mechanism, the enol-to-keto tautomerization is the RDS, with an activation Gibbs free energy of $\Delta G^{\ddagger}_{298}$ = 68.6 kcal mol^{-1} relative to the DGP reactant.
3. In the catalyzed mechanism, the enol-to-keto tautomerization has a reaction barrier of $\Delta G^{\ddagger}_{298}$ = 53.5 kcal mol^{-1} and is no longer the RDS. In this scenario, the ring-opening hydration step becomes the RDS, with a barrier of $\Delta G^{\ddagger}_{298}$ = 58.1 kcal mol^{-1}; this barrier is closely followed by the barrier for the ring-opening hydrogen-transfer step ($\Delta G^{\ddagger}_{298}$ = 57.3 kcal mol^{-1}).
4. The transformation from DGP to LGO is thermodynamically favoured as the Gibbs free energy of LGO lies 11.6 kcal mol^{-1} below DGP.

Our results provide important insights into the molecular mechanisms of biomass pyrolysis. Most notably that this conversion is water-catalyzed and that the ring-opening hydration step is the RDS. We hope that our high-level theoretical results will inspire additional experimental measurements.

Supplementary Material

Gibbs free energies for the first step in the competing reaction mechanism proposed by Shafizadeh et al.[26] (Table S1 and Fig. S1); G4(MP2) reaction profile on the enthalpic surface for the uncatalyzed and water-catalyzed conversion of DGP into LGO, including zero-point vibrational energy (ZPVE), heat content function (H_{298}–H_0), and entropic (ΔS) corrections from G4(MP2) theory (Table S2); absolute energies required to

calculate all the data in Table S2 (Table S3); and B3LYP/6–31G (2df,p) optimized geometries for all the local minima and transition structures considered in this work (Table S4) are available on the Journal's website.

Acknowledgements

This study is dedicated to the late Professor Allan H. White (1938–2016) who made numerous contributions to the fields of inorganic chemistry and crystallography.[53] This research was undertaken with the assistance of resources from the National Computational Infrastructure (NCI), which is supported by the Australian Government. We also acknowledge system administration support provided by the Faculty of Science at University of Western Australia to the Linux cluster of the Karton group. We gratefully acknowledge the provision of a Scholarship for International Research Fees (SIRF) and a University International Stipend scholarship (to W.W.), the provision of an Australian Postgraduate Award (to L.-J.Y.), and an Australian Research Council (ARC) Discovery Early Career Researcher Award (to A.K.; Project No. DE140100311).

References

[1] W. de Jong, in *Biomass as a Sustainable Energy Source for the Future* (Ed. W. de Jong, V. O. J. Ruud) **2014**, Ch. 15, pp. 469–502 (John Wiley & Sons, Inc.: Hoboken, NJ).

[2] M. Parikka, *Biomass Bioenergy* **2004**, *27*, 613. doi:10.1016/J.BIOMBIOE.2003.07.005

[3] A. V. Bridgwater, G. V. C. Peacocke, *Renewable Sustainable Energy Rev.* **2000**, *4*, 1. doi:10.1016/S1364-0321(99)00007-6

[4] J. P. Diebold, *A Review of the Chemical and Physical Mechanisms of the Storage Stability of Fast Pyrolysis Bio-Oils* **2000** (National Renewable Energy Laboratory: Lakewood, CO).

[5] O. D. Mante, F. A. Agblevor, *Waste Manage.* **2012**, *32*, 67. doi:10.1016/J.WASMAN.2011.09.004

[6] A. Oasmaa, E. Kuoppala, Y. Solantausta, *Energy Fuels* **2003**, *17*, 433. doi:10.1021/EF020206G

[7] F. Shafizadeh, R. H. Furneaux, T. T. Stevenson, *Carbohydr. Res.* **1979**, *71*, 169. doi:10.1016/S0008-6215(00)86069-3

[8] P. Bhaté, D. Horton, *Carbohydr. Res.* **1983**, *122*, 189. doi:10.1016/0008-6215(83)88330-X

[9] K. Matsumoto, T. Ebata, H. Matsushita, *Carbohydr. Res.* **1995**, *279*, 93. doi:10.1016/0008-6215(95)00261-8

[10] Z. J. Witczak, R. Chhabra, H. Chen, X.-Q. Xie, *Carbohydr. Res.* **1997**, *301*, 167. doi:10.1016/S0008-6215(97)00100-6

[11] Y.-C. Lin, J. Cho, G. A. Tompsett, P. R. Westmoreland, G. W. Huber, *J. Phys. Chem. C* **2009**, *113*, 20097. doi:10.1021/JP906702P

[12] G. Dobele, T. Dizhbite, G. Rossinskaja, G. Telysheva, D. Meier, S. Radtke, O. Faix, *J. Anal. Appl. Pyrolysis* **2003**, *68–69*, 197. doi:10.1016/S0165-2370(03)00063-9

[13] G. Dobele, G. Rossinskaja, T. Dizhbite, G. Telysheva, D. Meier, O. Faix, *J. Anal. Appl. Pyrolysis* **2005**, *74*, 401. doi:10.1016/J.JAAP.2004.11.031

[14] Z.-B. Zhang, Q. Lu, X.-N. Ye, T.-P. Wang, X.-H. Wang, C.-Q. Dong, *BioEnergy Res.* **2015**, *8*, 1263. doi:10.1007/S12155-015-9581-6

[15] X.-W. Sui, Z. Wang, B. Liao, Y. Zhang, Q.-X. Guo, *Bioresour. Technol.* **2012**, *103*, 466. doi:10.1016/J.BIORTECH.2011.10.010

[16] S. Kudo, Z. Zhou, K. Norinaga, J.-I. Hayashi, *Green Chem.* **2011**, *13*, 3306. doi:10.1039/C1GC15975E

[17] Z. Wang, Q. Lu, X.-F. Zhu, Y. Zhang, *ChemSusChem* **2011**, *4*, 79. doi:10.1002/CSSC.201000210

[18] Y. Halpern, R. Riffer, A. Broido, *J. Org. Chem.* **1973**, *38*, 204. doi:10.1021/JO00942A005

[19] R. S. Assary, L. A. Curtiss, *ChemCatChem* **2012**, *4*, 200. doi:10.1002/CCTC.201100280

[20] Q. Lu, Y. Zhang, C.-q. Dong, Y.-P. Yang, H.-Z. Yu, *J. Anal. Appl. Pyrolysis* **2014**, *110*, 34. doi:10.1016/J.JAAP.2014.08.002

[21] P. R. Patwardhan, J. A. Satrio, R. C. Brown, B. H. Shanks, *J. Anal. Appl. Pyrolysis* **2009**, *86*, 323. doi:10.1016/J.JAAP.2009.08.007

[22] Q. Lu, X.-C. Yang, C.-Q. Dong, Z.-F. Zhang, X.-M. Zhang, X.-F. Zhu, *J. Anal. Appl. Pyrolysis* **2011**, *92*, 430. doi:10.1016/J.JAAP.2011.08.006

[23] M. S. Mettler, A. D. Paulsen, D. G. Vlachos, P. J. Dauenhauer, *Green Chem.* **2012**, *14*, 1284. doi:10.1039/C2GC35184F

[24] J. C. Degenstein, P. Murria, M. Easton, H. Sheng, M. Hurt, A. R. Dow, J. Gao, J. J. Nash, R. Agrawal, W. N. Delgass, F. H. Ribeiro, H. I. Kenttämaa, *J. Org. Chem.* **2015**, *80*, 1909. doi:10.1021/JO5025255

[25] A. M. Sarotti, *Carbohydr. Res.* **2014**, *390*, 76. doi:10.1016/J.CARRES.2014.03.017

[26] F. Shafizadeh, R. H. Furneaux, T. T. Stevenson, T. G. Cochran, *Carbohydr. Res.* **1978**, *60*, 519. doi:10.1016/S0008-6215(00)83614-9

[27] L. A. Curtiss, P. C. Redfern, K. Raghavachari, *J. Chem. Phys.* **2007**, *127*, 124105. doi:10.1063/1.2770701

[28] W. J. Hehre, L. Radom, P. R. Schleyer, J. A. Pople, *Ab Initio Molecular Orbital Theory* **1986** (Wiley: New York).

[29] W. Koch, M. C. Holthausen, *A Chemist's Guide to Density Functional Theory* **2001** (Wiley-VCH Verlag GmbH).

[30] M. J. Frisch, G. W. Trucks, H. B. Schlegel, G. E. Scuseria, M. A. Robb, J. R. Cheeseman, G. Scalmani, V. Barone, B. Mennucci, G. A. Petersson, H. Nakatsuji, M. Caricato, X. Li, H. P. Hratchian, A. F. Izmaylov, J. Bloino, G. Zheng, J. L. Sonnenberg, M. Hada, M. Ehara, K. Toyota, R. Fukuda, J. Hasegawa, M. Ishida, T. Nakajima, Y. Honda, O. Kitao, H. Nakai, T. Vreven, J. A. Montgomery Jr, J. E. Peralta, F. Ogliaro, M. J. Bearpark, J. Heyd, E. N. Brothers, K. N. Kudin, V. N. Staroverov, R. Kobayashi, J. Normand, K. Raghavachari, A. P. Rendell, J. C. Burant, S. S. Iyengar, J. Tomasi, M. Cossi, N. Rega, N. J. Millam, M. Klene, J. E. Knox, J. B. Cross, V. Bakken, C. Adamo, J. Jaramillo, R. Gomperts, R. E. Stratmann, O. Yazyev, A. J. Austin, R. Cammi, C. Pomelli, J. W. Ochterski, R. L. Martin, K. Morokuma, V. G. Zakrzewski, G. A. Voth, P. Salvador, J. J. Dannenberg, S. Dapprich, A. D. Daniels, Ö. Farkas, J. B. Foresman, J. V. Ortiz, J. Cioslowski, D. J. Fox, *Gaussian 09* **2009** (Gaussian, Inc.; Wallingford, CT).

[31] C. Gonzalez, H. B. Schlegel, *J. Chem. Phys.* **1989**, *90*, 2154. doi:10.1063/1.456010

[32] C. Gonzalez, H. B. Schlegel, *J. Phys. Chem.* **1990**, *94*, 5523. doi:10.1021/J100377A021

[33] L. A. Curtiss, P. C. Redfern, K. Raghavachari, *J. Chem. Phys.* **2007**, *126*, 084108. doi:10.1063/1.2436888

[34] L. A. Curtiss, P. C. Redfern, K. Raghavachari, *Wiley Interdiscip. Rev.: Comput. Mol. Sci.* **2011**, *1*, 810. doi:10.1002/WCMS.59

[35] A. Karton, *Wiley Interdiscip. Rev.: Comput. Mol. Sci.* **2016**, *6*, 292. doi:10.1002/WCMS.1249

[36] L. A. Curtiss, P. C. Redfern, K. Raghavachari, *J. Chem. Phys.* **2005**, *123*, 124107. doi:10.1063/1.2039080

[37] L. A. Curtiss, P. C. Redfern, K. Raghavachari, *Chem. Phys. Lett.* **2010**, *499*, 168. doi:10.1016/J.CPLETT.2010.09.012

[38] A. Karton, R. J. O'Reilly, L. Radom, *J. Phys. Chem. A* **2012**, *116*, 4211. doi:10.1021/JP301499Y

[39] A. Karton, L. Goerigk, *J. Comput. Chem.* **2015**, *36*, 622. doi:10.1002/JCC.23837

[40] L.-J. Yu, F. Sarrami, R. J. O'Reilly, A. Karton, *Chem. Phys.* **2015**, *458*, 1. doi:10.1016/J.CHEMPHYS.2015.07.005

[41] A. Karton, *Chem. Phys. Lett.* **2014**, *592*, 330. doi:10.1016/J.CPLETT.2013.12.062

[42] G. da Silva, *Angew. Chem., Int. Ed.* **2010**, *49*, 7523. doi:10.1002/ANIE.201003530

[43] A. Karton, J. M. L. Martin, *J. Chem. Phys.* **2012**, *136*, 124114. doi:10.1063/1.3697678

[44] R. S. Assary, P. C. Redfern, J. Greeley, L. A. Curtiss, *J. Phys. Chem. B* **2011**, *115*, 4341. doi:10.1021/JP1104278

[45] A. Karton, R. J. O'Reilly, B. Chan, L. Radom, *J. Chem. Theory Comput.* **2012**, *8*, 3128. doi:10.1021/CT3004723

[46] L. Vereecken, J. S. Francisco, *Chem. Soc. Rev.* **2012**, *41*, 6259. doi:10.1039/C2CS35070J

[47] E. Vöhringer-Martinez, B. Hansmann, H. Hernandez, J. S. Francisco, J. Troe, B. Abel, *Science* **2007**, *315*, 497. doi:10.1126/SCIENCE.1134494

[48] V. Minkova, M. Razvigorova, E. Bjornbom, R. Zanzi, T. Budinova, N. Petrov, *Fuel Process. Technol.* **2001**, *70*, 53. doi:10.1016/S0378-3820(00)00153-3

[49] V. Minkova, M. Razvigorova, M. Goranova, L. Ljutzkanov, G. Angelova, *Fuel* **1991**, *70*, 713. doi:10.1016/0016-2361(91)90067-K

[50] J. Scheirs, G. Camino, W. Tumiatti, *Eur. Polym. J.* **2001**, *37*, 933. doi:10.1016/S0014-3057(00)00211-1

[51] W. Plazinski, A. Plazinska, M. Drach, *Phys. Chem. Chem. Phys.* **2015**, *17*, 21622. doi:10.1039/C5CP03357H

[52] R. S. Assary, L. A. Curtiss, *Energy Fuels* **2012**, *26*, 1344. doi:10.1021/EF201654S

[53] G. Koutsantonis, Y. Kim, *Aust. J. Chem.* **2012**, *65*, 695. doi:10.1071/CH12304